XVIII IMEKO WORLD CONGRESS
Metrology for a Sustainable Development
September, 17 – 22, 2006, Rio de Janeiro, Brazil

NEW METHOD FOR INWARD LEAKAGE DETECTION

Ales Hribernik [1], *Gorazd Bombek* [1]

[1] University of Maribor, Maribor, Slovenia, ales.hribernik@uni-mb.si

Abstract: A new non-destructive method was developed for the detection of refrigerant leakage at an evaporator's inflow. Nitrogen and oxygen gas were blown through the evaporator in successive time intervals. A gas analyser was applied at the outflow of the evaporator and the oxygen concentration measured. It was possible to detect any leakage by investigating the oxygen concentration-time history diagram.

Keywords: leakage detection, refrigeration, plate evaporator

1. INTRODUCTION

Plate evaporators are commonly used in household refrigerators. They form an inner-wall and a source of cooling, at the same time. A plate evaporator consists of two aluminium sheets coupled together by a special pressing process, in such a way as to form a system of small channels and caverns. The evaporator is fed with refrigerant through a capillary tube. In order to minimize any leakage of refrigerant out of the system and into the ambient, the capillary tube is placed coaxial into the evaporator outflow pipe, and is connected to the evaporator inflow using a press joint (Fig. 1). Therefore, the leakage of this joint does not contribute to any loss of refrigerant into the ambient, and thus very high sealing standards can be achieved.

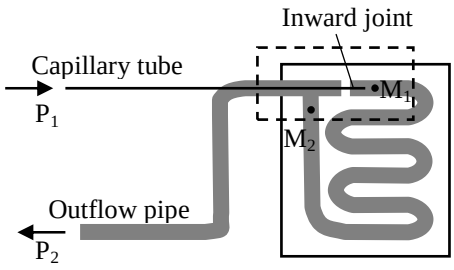

Fig. 1: Plate evaporator

1.1. *Inward leakage of refrigerant*

The plate evaporator is schematically shown in Fig. 1. As can be seen, the capillary tube is placed coaxially within the outflow tube, and inwardly connected to the evaporator. Under normal operational procedure the freshly condensed refrigerant should flow into the evaporator, fill its channels and caverns, cool the evaporator by evaporation and, finally, be sucked out by the compressor and leave the evaporator. When, however, the joint between the capillary tube and evaporator leaks, one part of the condensed refrigerant flows directly into the outflow. The cooling capacity of the evaporator is, therefore, reduced thus hindering the normal operation of the refrigerator.

1.2. *Conditions within the inward joint*

Leakage intensity is influenced by the size and form of the gap between the capillary and the evaporator, and by any pressure drop across the joint (pressure difference between M1 and M2 – Fig. 1). The size and form of the gap both depend on the quality of the joint pressing tool and do not change over time, whilst the pressure drop varies during the refrigerator's operation. Two piezo-resistive transducers were used and mounted on a plate evaporator next to M1 and M2 (Fig. 1) in order to measure any pressure traces during an ordinary refrigerator's cooling system operation. Fig. 2 shows typical pressure traces and calculated pressure drop across the joint. It reaches its peak during the compressor operation and drops to zero when the compressor is switched off. The maximum pressure drop measured during operation was 30 kPa and coincided with the start of compressor. The mean pressure drop during compressor operation was 20 kPa. Even the thinnest gap could cause considerable refrigerant leakage under these circumstances, since the operation of the compressor lasted 30 minutes.

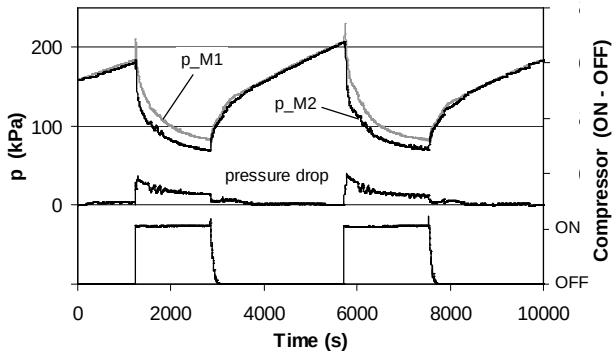

Fig. 2: Pressure traces at M1 and M2 during operation of the refrigerator

1.3. *Common leakage detection method*

As stated previously, the leakage of refrigerant at the evaporator's inflow causes malfunction of the refrigerator and, therefore, must normally be controlled.

A destructive method is commonly used to check the quality of any inward joint of the capillary tube and evaporator. The marked area shown in Fig. 1 is simply cut-out of the evaporator and the opening M2 is sealed. Compressed air is then applied on the outflow pipe, the joint is immersed in the water and inspected for possible leakage. A small leakage is permissible, otherwise the production line is stopped until the joint leakage is annulated. All the evaporators produced after the last successful control, are removed from the production line, since they can not be individually checked without destruction.

A new non-destructive method for leakage detection was developed which could be simply incorporated into the production line and every individual plate evaporator could then be checked.

2. NON-DESTRUCTIVE METHOD FOR LEAKAGE DETECTION

All the evaporators have to be checked for inward leakage so it is necessary to apply a non-destructive method. A successful leakage detection method could reduce the number of rejected evaporators significantly.

2.1. Idea

Small particles (molecules) of fluid flow through the evaporator, travel from the capillary tube inflow P1 (Fig. 1), pass the joint M1, meander through the channels of the evaporator, pass the junction M2, and exit the outflow pipe at P2. The passage time depends on the average speed of particles and the length of the course. When the joint leaks, one section of the molecules passes directly from M1 to M2 and their passage time reduces significantly. Detection of reduced passage time, therefore, indicates any leakage of the joint. The problem occurs, however, when attempting to mark the observed particles. The application of two different gasses may overcome this problem very effectively. The idea is to blow the system through using an inert gas over a specified time and then, at a pre-selected moment replace the inert gas by an active one, which could then be detected by a gas analyser. The passage time of the active gas could then be determined simply from the time history of the gas analyser's signal.

2.2. Measuring system design

The measuring system consists of a gas commutator and a gas analyser, connected to the tested evaporator (Fig. 3). The task of the gas commutator is to enable fast commutation of inert and active gasses. The gas analyser has to detect active gas at a very low concentration and has to have a very fast impulse response.

2.2.1. Gas commutator

The gas commutator has to ensure a fast commutation of gases without mixing, and an instantaneous delivery of the active gas at its highest concentration level (an expressive rise of active gas concentration is demanded). Different designs were tested and the final design is shown in Fig 4. This gas commutator is composed of a narrow gas chamber connected to the supplies of inert and active gas by solenoid valves. The operation of solenoid valves is actuated by a relay which is controlled by a computer through a multifunction I/O card. The third solenoid valve is applied to blow out the gas chamber after the evaporator has been connected to the gas commutator.

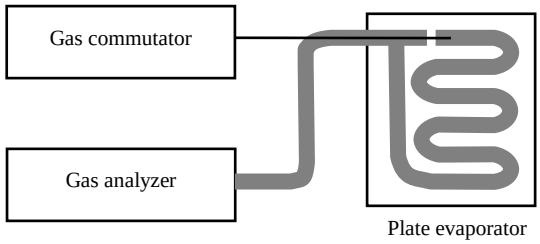

Fig. 3: Measuring system

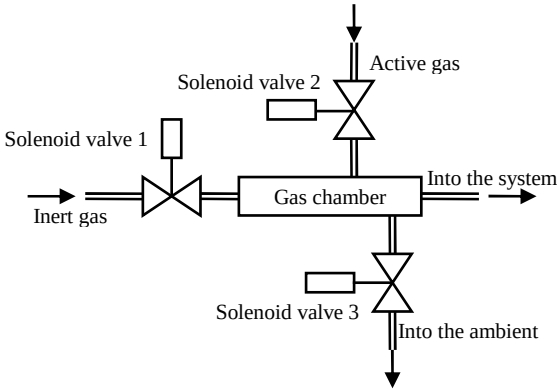

Fig. 4: Gas commutator

2.2.2 Gas analyser

Different gasses were considered as the active gas. It has to be highly detectable, operationally safe, and in accordance with production demands (non-organic or inflammable gas). Oxygen was selected as the active gas after studying different gas analysers, and a ZrO_2 sensor was applied for oxygen detection. This type of a sensor is very sensitive at low oxygen concentration and reacts very quickly to sudden abrupt changes in oxygen concentration. The electrical voltage signal from the sensor is proportional to the logarithm of the ambient and sample oxygen partial pressure ratio, and can be calculated by Nernst's equation [1]

$$U = \frac{R_m T}{4F} \ln\left(\frac{p_{O_2,amb}}{p_{O_2,sample}}\right) \quad (1)$$

As can be seen the voltage U is proportional to the temperature which dictates the rate of oxygen ions flow through ZrO_2. The dependence of Nernst's voltage on temperature is shown in Fig. 5. The sensitivity at 1000 K is 70 % higher than that at 600 K. The temperature has, therefore, to be held well-above room temperature for higher sensor sensitivity. In order to take advantage of this fact, the sensor was placed into an electrically heated chamber (Fig. 6) where the sample gas was heated to 1400 K.

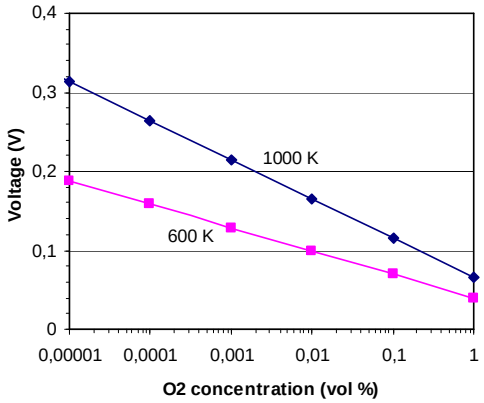

Fig. 5: The dependence of Nernst's voltage on temperature

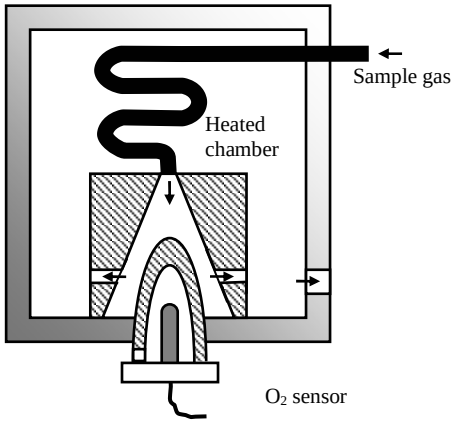

Fig. 6: Sample and sensor heating

2.2.3 Operation of the system

The automatic computer-controlled testing procedure is started after the capillary tube of the evaporator is connected to the gas commutator and the outflow tube to the oxygen analyser. The nitrogen gas is switched on and the oxygen concentration in the out flowing gas is measured. Being replaced by the nitrogen, the oxygen concentration slowly falls and the electrical signal from the oxygen sensor rises (Fig. 7). Once the rise of the signal is terminated - no oxygen is detected and the commutator automatically switches off the nitrogen and, simultaneously, switches on the oxygen. After a certain time-interval necessary for the gas to travel through the evaporator, the oxygen concentration rises and the signal from the sensor reduces. The oxygen is switched off and the results are processed.

In order to determine the passage time, the oxygen sensor signal trace within the interval of interest (see Fig. 7) has to be acquired and analysed. The acquisition of a signal is triggered by the control signal of the oxygen solenoid valve. This assures a very accurate time-base, and a high resolution of time scale.

The passage time is determined from the signal-trace, as shown in Fig. 8. It measures the time interval between switching on the oxygen solenoid valve and sudden signal decline (passing of the 0.4 V limit). Two curves are presented in Fig. 1. Both were measured using the same type of evaporator, but exhibited different leakages (0% and 4.3 %). The difference between both passage times is obvious, thus the detection of leakage is straightforward.

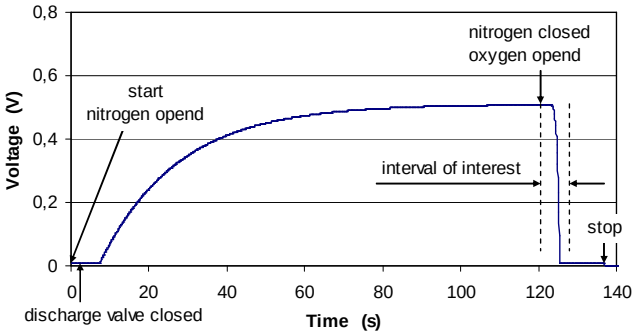

Fig. 7: Oxygen sensor signal time history

The computer application was programmed in LabWIEV 6.1 programming language product from National Instruments [2].

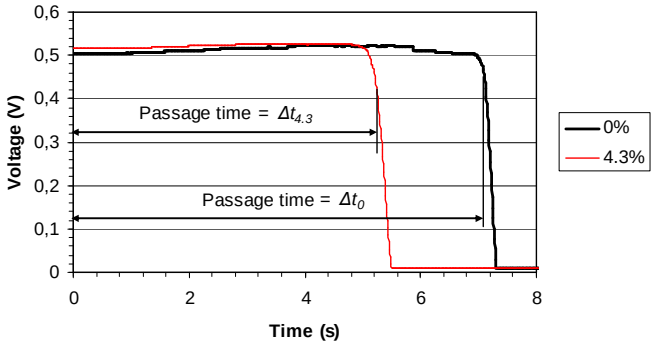

Fig. 8: Determination of passage time (0% and 4.3% leakage)

3. SYSTEM CALIBRATION

As already shown any reduction in passage time occurs when the inspected inward joint leaks. The main task of calibration was, therefore, to determine any correlation between leak intensity and passage time reduction. A model of a plate evaporator was created, which allowed leak intensity to be controlled for the purpose of system calibration.

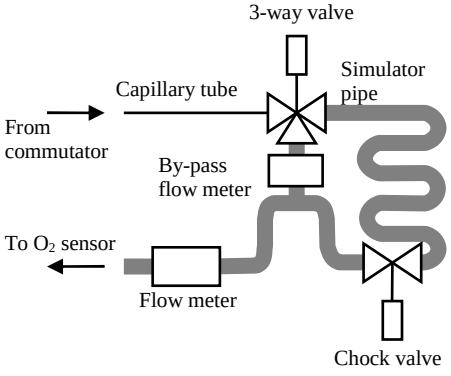

Fig. 9: Schematics of evaporator model

The evaporator model is schematically shown in Fig. 9. The capillary tube is interconnected through a 3-way valve to the main simulator pipe, which corresponds to the

channels of the evaporator. Both have the same flow characteristics, i.e. the same length, hydraulic diameter and pressure drop. The latter can be finely adjusted by a needle valve mounted on the main simulator pipe and has to be measured for each type of inspected evaporators under testing conditions (pressure at the capillary tube inflow P1 – Fig. 1). Pressure drop, as measured by blowing compressed nitrogen through the evaporator under different conditions, and measuring the pressure difference between M1 and M2 (see Fig. 1), is shown in Fig. 10. As can be seen, a much higher pressure drop was measured under refrigerator operating conditions (Fig. 2), when system operated using refrigerant.

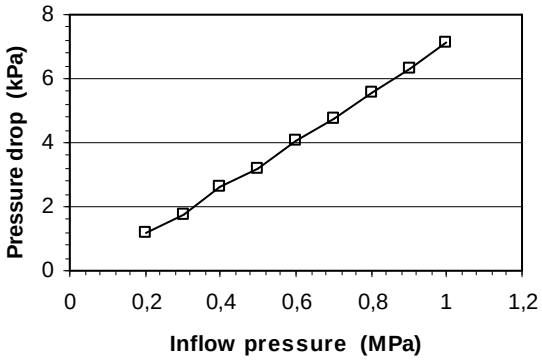

Fig. 10: The dependence of pressure drop of plate evaporator on flow conditions (pressure of nitrogen at the capillary tube inflow P1)

Leakage simulation is established by a by-pass which interconnects the far-end of the main simulator pipe with the third connector of the 3-way valve, the effective flow area of which could be adjusted from no leakage when closed to 100% leakage when fully opened. Both the main and leakage flows were simultaneously measured using a laminar flow meter, and leakage intensity was calculated as

$$I_{leak} = \frac{\dot{V}_{leak}}{\dot{V}_{main}}, \qquad (2)$$

which was correlated with the passage time. Instead of passage time, a relative advance-time defined as

$$T_{a,r} = \frac{\Delta t_0 - \Delta t}{\Delta t_0}, \qquad (3)$$

was applied, where Δt_0 was the passage time when no leakage was presented ($I_{leak} = 0$).

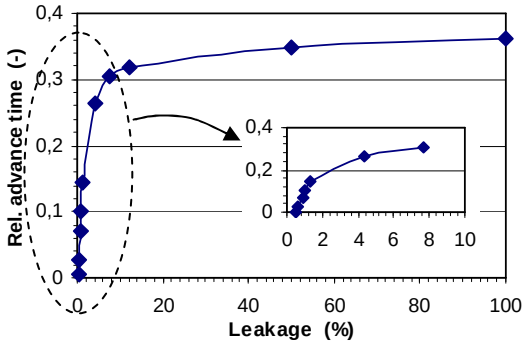

Fig. 11: Calibration results

Typical calibration results are presented in Fig. 11. Advance time increases with leakage very quickly in the low to moderate leakage range. Once the leakage exceeds 10 % the advance time increases very slowly, and reaches 0.36 at 100 % leakage, which is the relative time for passing the evaporator. The very high sensitivity of the system within the low leakage range makes leakage detection effective at 1 % or higher leakage. For the prediction of leakage intensity, however, it is necessary to determine a calibration curve. This is presented in Fig. 12. When plotted as $\ln I_{leak}$ against relative advance time $T_{a,r}$, the calibration curve becomes almost a straight line, which can be easily extrapolated by an exponential function with multiplication constant, corresponding to the minimum detectable leakage. This was 0.46% for the inspected evaporator.

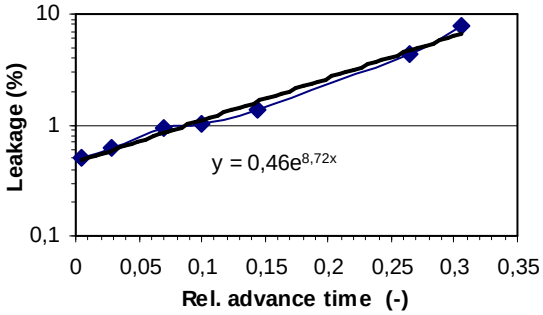

Fig. 12: Calibration curve

4. EVAPORATOR TESTINGS

Specially designed evaporators were used for testing the presented method. Different leakage intensity was achieved by the reduction of the amount of sealant glue applied, when joining the capillary tube to evaporator. Evaporators were then classified into 3 groups: without sealant glue, with a common amount of glue, and with an overdosed amount of glue. Essential leakage was expected for the first group of evaporators, reduced leakage for the second group and no leakage for the third. After calibration had been completed, tests using the evaporators were performed. Fig 13 shows a comparison of the results obtained for the first (essential leakage) and third (no leakage) groups.

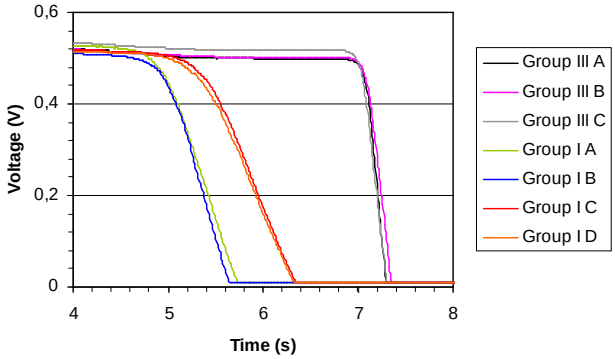

Fig. 13: Comparison of tests performed for the first (essential leakage) and third (no leakage) group of evaporators

The curves for the third group of evaporators grouped together very well. All evaporators from this group sealed 100% as was proved by the common destructive test after

performing the non-destructive method. The small scatter is due to the tolerances of the diameter and length of the capillary tube. The first group was distributed well-ahead of the third, with a much greater scatter, which suggested different leakage intensity for each individual evaporator. Applying the calibration curve the leakage intensity I_{leak} of the first group was predicted to be between 3 to 5 %.

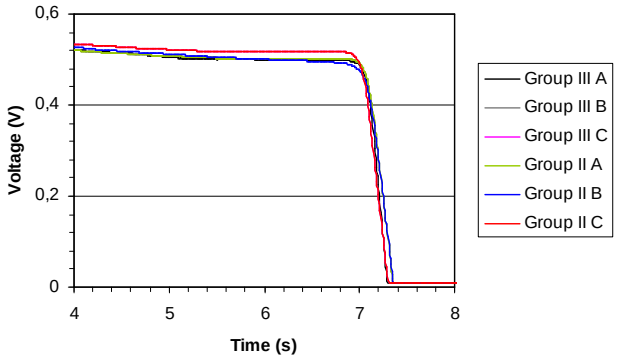

Fig. 14: Comparison of tests performed for the second (low leakage) and third (no leakage) group of evaporators

A comparison of the results obtained for the second (low leakage) and third (no leakage) group of evaporators was less promising (Fig. 14). All the curves were grouped together and no reliable separation was possible. The only suggestion was that the leakage was well below the detection limit, which was as stated by calibration 0.5 % (Fig. 12). The common destructive test proved this assumption, since the leakage for the second evaporator group of evaporators predicted by this method was between 0.05 and 0.1 %. At these low-leakages the change of oxygen concentration was too low to be detected by the applied oxygen sensor. More sensitive sensors would probably do the job, however, there would still exist some scatter due to the production tolerances, which would reduce the reliability of the system within the extreme low leakage range.

5. CONCLUSIONS

A new method is presented for the detection of plate evaporator inward leakage. This method is non-destructive, which is its main advantage over existing methods. The procedure is fast and can be effectively incorporated into the production line of plate evaporators in order to check them before their application in the refrigerators. This method was extensively tested and showed very high reliability. The minimum detectable leakage was 0.5 % of the main gas flow. It is expected that this limit can be further reduced by the application of more sensitive oxygen sensors.

REFERENCES

[1] Petanides, K., Marincek, B., Heimke, G., Messen des freien Sauerstoffs, Chemie-anlagen + Verfahren, Heft 6/1973, pp. 167-169

[2] LabVIEW – User Manual, National Instruments Corporation, Austin, Texas, USA, 2000